Supplementary Information

PAF-1@Cellulose Nanofibril Composite Aerogel for Highly-efficient Removal of Bisphenol A

Danyang Zhao, [a] Yuyang Tian, [a] Xiaofei Jing, *[a] Yun Lu, *[b] and Guangshan Zhu[a]

[a]Key Laboratory of Polyoxometalate Science of Ministry of Education, Northeast Normal University, Changchun 130024, P. R. China.

[b]Research Institute of Wood Industry, Chinese Academy of Forestry, Yard 1, Dongxiaofu, Xiangshan Road, Haidian District, Beijing 100091, P.R. China.

*E-mail: jingxf100@nenu.edu.cn; y.lu@caf.ac.cn

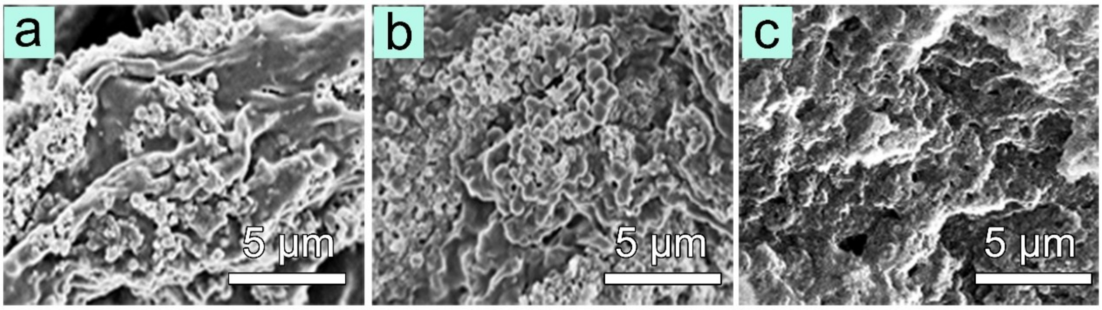

Fig. S1 SEM images of PAF-1@CNF composite aerogels with the PAF-1 content of (a) 20 wt%, (b) 33.3%, and (c) 50 wt%.

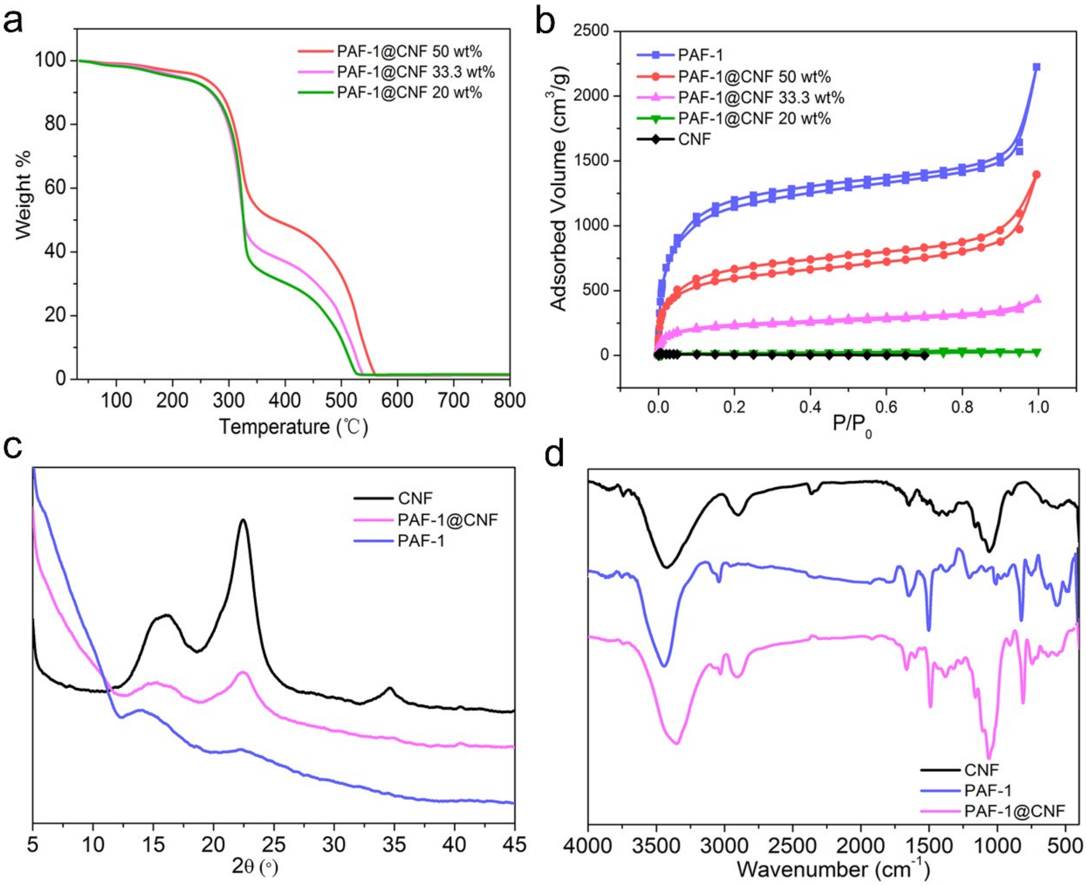

Fig. S2 (a) TGA curves for PAF-1@CNF composite aerogels with PAF-1 content of 20, 33.3, and 50 wt%. (b) Nitrogen adsorption-desorption isotherms of double-cross-linked CNF aerogel, PAF-1, and PAF-1@CNF composites with the PAF-1 content of 20, 33.3, and 50 wt%. (c) XRD patterns of PAF-1, physically cross-linked CNF aerogel, and PAF-1@CNF composite aerogel with the PAF-1 content of 33.3 wt%. (d) FTIR spectra of PAF-1, physically cross-linked CNF aerogel, and PAF-1@CNF composite aerogel with PAF-1 content of 33.3 wt%.

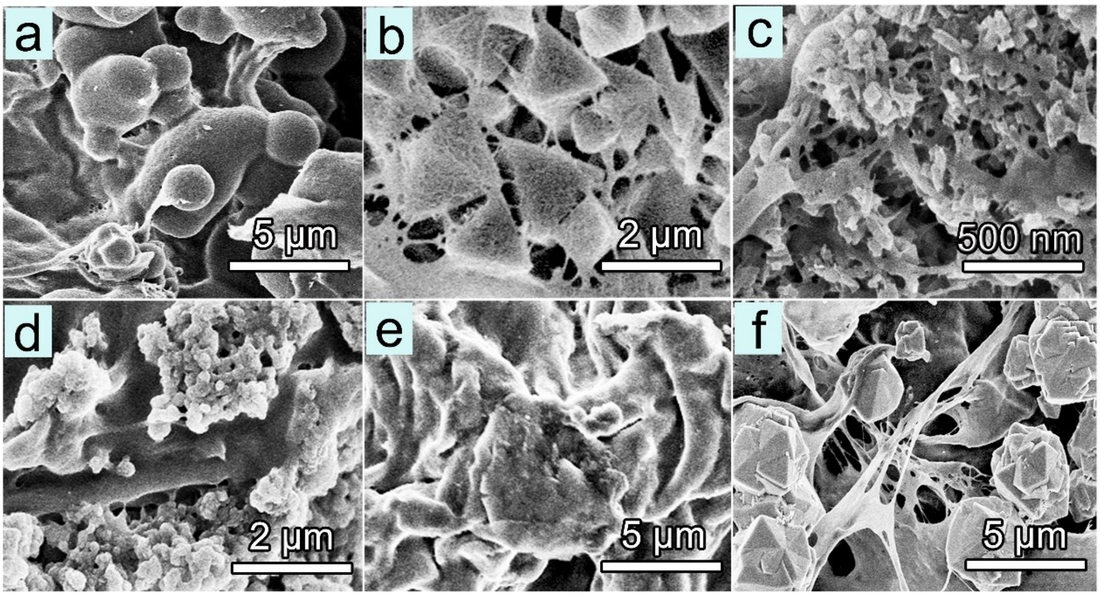

Fig. S3 SEM images of CNFs-based composite aerogels loaded with (a) PAF-45, (b) MIL-101, (c) MIL-53, (d) PIM-1, (e) activated carbon, and (f) zeolite-X.

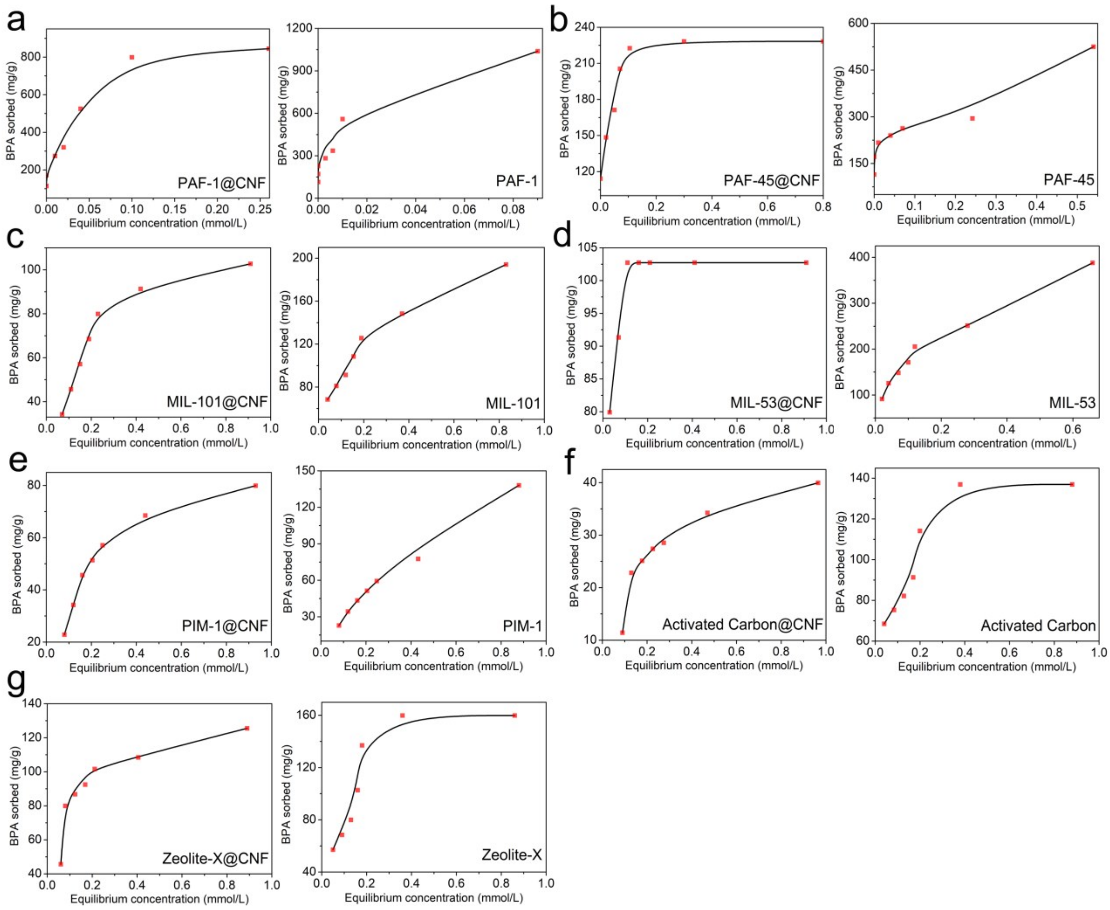

Fig. S4 Plot of the adsorption equilibrium uptake of CNF composite aerogels loaded with (a) PAF-1, (b) PAF-45, (c) MIL-101, (d) MIL-53, (e) PIM-1, (f) activated carbon, and (g) zeolite-X composite aerogels (left panels) and their corresponding powders (right panels) versus the initial concentration of BPA in water.

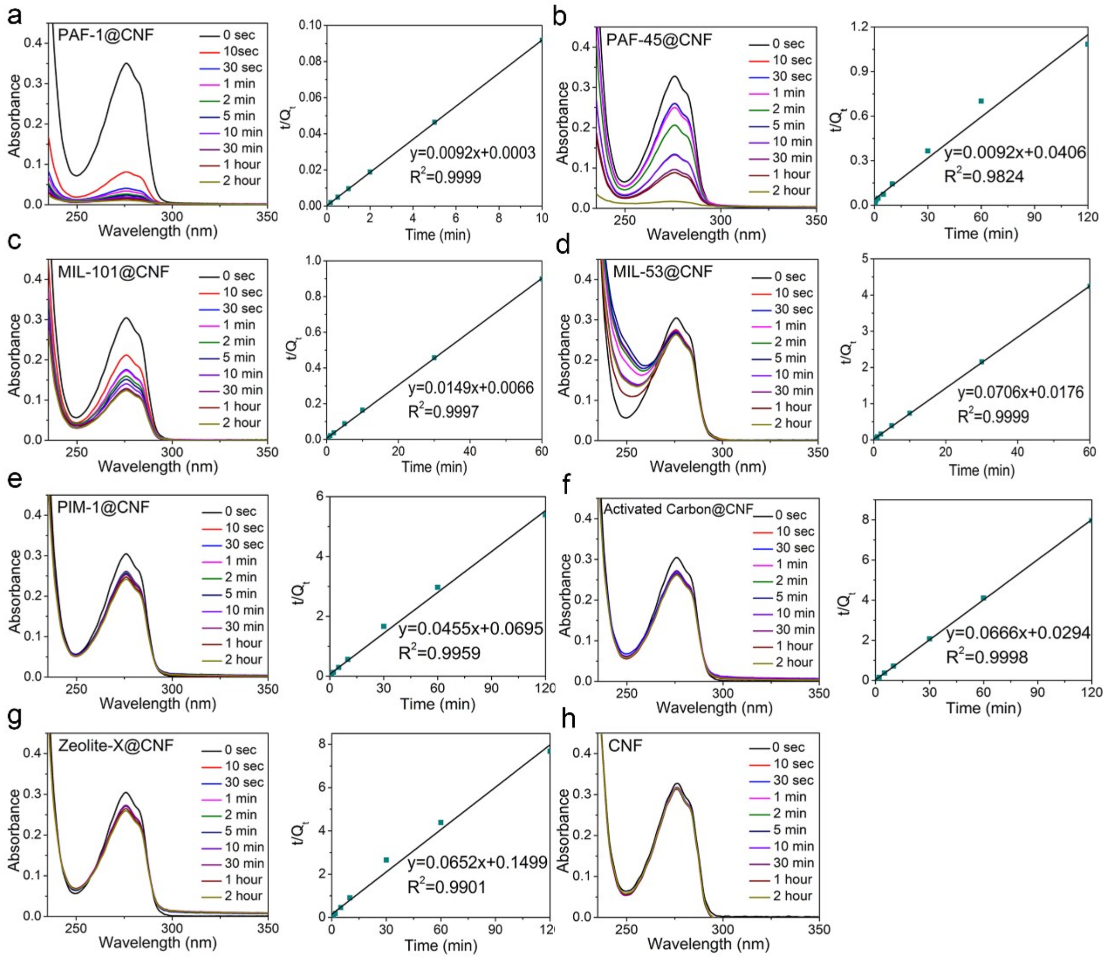

Fig. S5 Temporal evolution of the UV–vis spectra of the aqueous solution of BPA during adsorption of CNF composite aerogels loaded with (a) PAF-1, (b) PAF-45, (c) MIL-101, (d) MIL-53, (e) PIM-1, (f) activated carbon, and (g) zeolite-X, and (h) pristine CNF aerogel (left panels) and the pseudo-second-order plots (right panels) of the corresponding CNF composite.

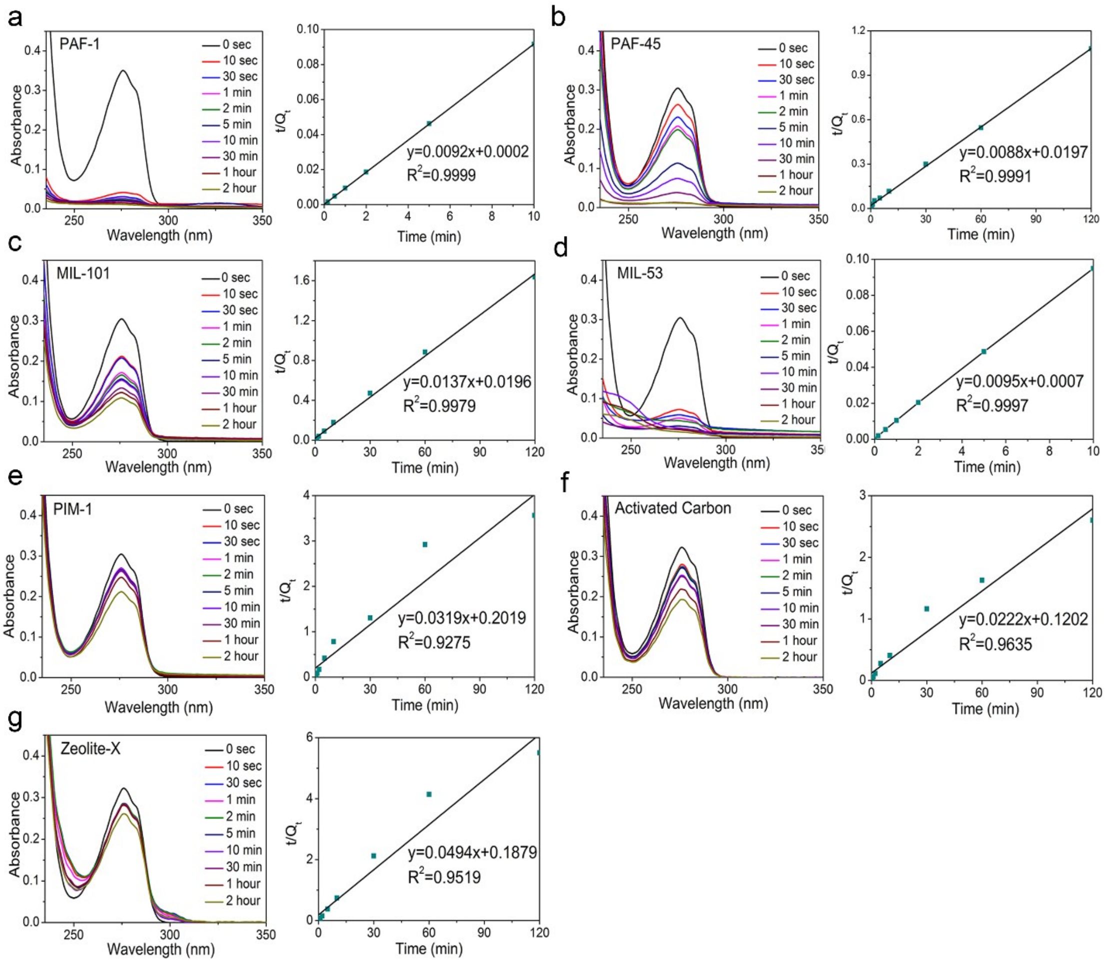

Fig. S6 Temporal evolution of the UV–vis spectra of the aqueous solution of BPA during adsorption of the powders of (a) PAF-1, (b) PAF-45, (c) MIL-101, (d) MIL-53, (e) PIM-1, (f) activated carbon, and (g) zeolite-X (left panels) and the pseudo-second-order plots (right panels) of the corresponding porous material powder.

Table S1 BET surface areas, maximum sorption capacities and BPA removal performance of CNF composite aerogels loaded with PAF-1, PAF-45, MIL-101, MIL-53, PIM-1, activated carbon, and zeolite-X and their corresponding porous materials.

Adsorbent	BET surface area (m^2 g^{-1})	Maximum sorption capacity (mg g^{-1})	%Removal efficiency		Time to reach equilibrium (min)	K_{obs} (g/ mg min)	Correlation coefficient R^2
			in 10 sec	in 1 h			
PAF-1@CNF	2203	1000	77.7	97.0	10	0.282	0.9999
PAF-1	4308	1428.6	89.2	97.0	10	0.423	0.9999
PAF-45@CNF	523	238.1	20.0	75.0	120	0.002	0.9824
PAF-45	1045	322.6	12.2	96.3	120	0.004	0.9991
MIL-101@CNF	2508	140.8	29.6	58.5	60	0.034	0.9997
MIL-101	2883	161.3	29.3	59.5	>120	0.010	0.9979
MIL-53@CNF	47	109.9	8.5	12.4	60	0.283	0.9999
MIL-53	1035	277.8	76.4	93.7	10	0.129	0.9997
PIM-1@CNF	17	135.1	13.1	17.7	120	0.030	0.9959
PIM-1	732	232.6	10.2	18.0	>120	0.005	0.9275
Activated carbon@CNF	30	65.4	9.5	12.8	120	0.151	0.9998
Activated carbon	704	125	12.9	32.3	>120	0.004	0.9635
Zeolite-X@CNF	35	144.9	9.2	12.0	>120	0.028	0.9901
Zeolite-X	672	185.2	11.1	12.7	>120	0.013	0.9519

Table S2 Structure, model, molecular weight, and charge of selected dyes and BPA.

No.	Dye	Structure	Model	M_w (g mol^{-1})	Charge
Dye-1	Acid red 94 (AR-94)	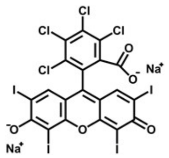	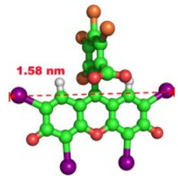	1017.63	-2
Dye-2	Brilliant blue G (BB-G)	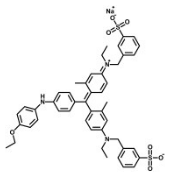	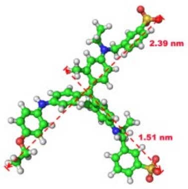	854.02	-1
Dye-3	Rhodamine B (R-B)	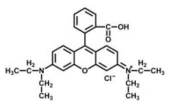	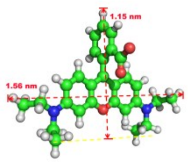	479.1	+1
Dye-4	Methylene blue (MB)	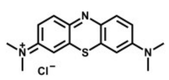		319.85	+1
5	Bisphenol A (BPA)	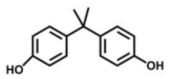	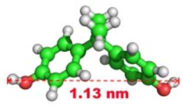	228.29	

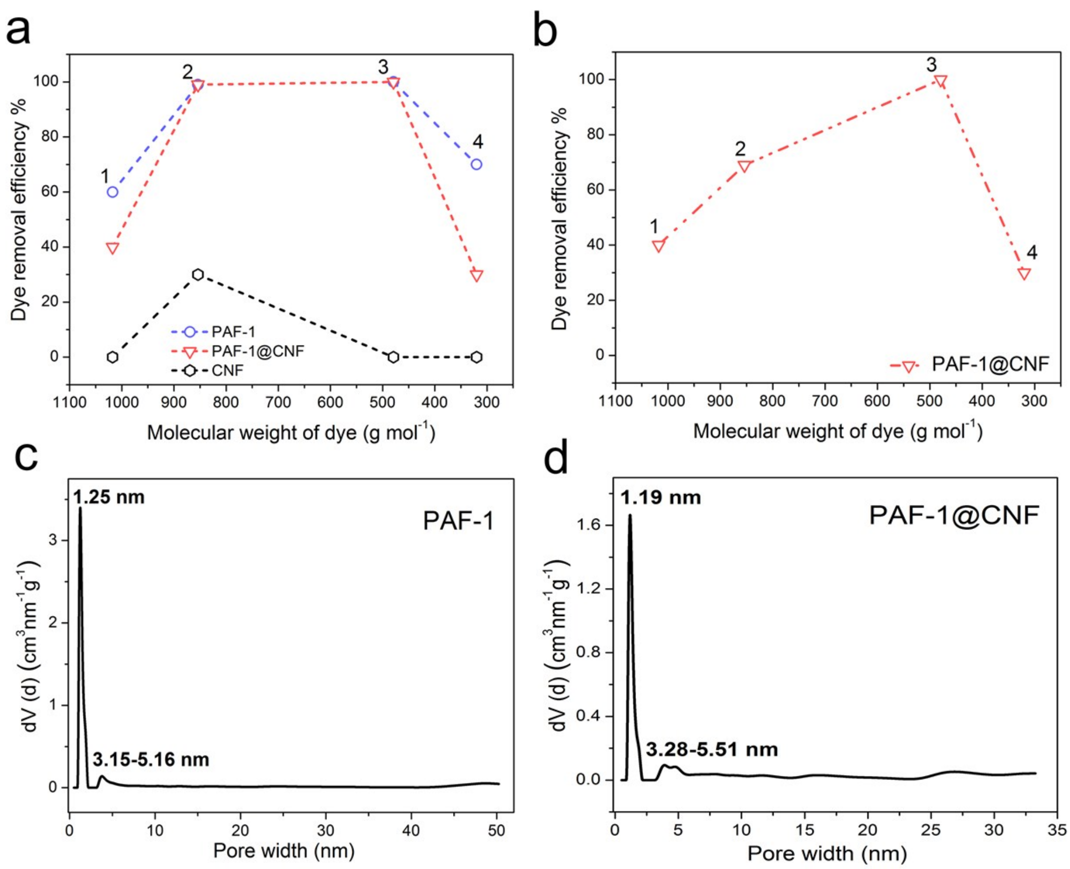

Fig. S7 (a) Dye removal efficiencies of different materials (PAF-1, PAF-1@CNF aerogel, and CNF aerogel) versus the molecular weight of selected dyes in water. (b) Dye removal efficiencies of PAF-1@CNF aerogel deducting CNF versus the molecular weight of dyes in water. Pore size distribution of (c) PAF-1 and (d) PAF-1@CNF aerogel.